Wave Based Method for Free Vibration Analysis of Cylindrical Shells With Nonuniform Stiffener Distribution

Jianhui Wei

Meixia Chen[1]
e-mail: chemx26@hust.edu.cn

Guoxiang Hou

Kun Xie

Naiqi Deng

School of Naval Architecture and Ocean Engineering, Huazhong University of Science and Technology, Wuhan 430074, China

Wave based method (WBM) is presented to analysis the free vibration characteristics of cylindrical shells with nonuniform stiffener distributions for arbitrary boundary conditions. The stiffeners are treated as discrete elements. The equations of motion of annular circular plate are used to describe the motion of stiffeners. Instead of expanding the dynamic field variables in terms of polynomial approximation in element based method (finite element method etc), the ring-stiffened cylindrical shell is divided into several substructures and the dynamic field variables in each substructure are expressed as wave function expansions. Boundary conditions and continuity conditions between adjacent substructures are used to form the final matrix to be solved. Natural frequencies of cylindrical shells with uniform rings spacing and eccentricity distributions for shear diaphragm-shear diaphragm boundary conditions have been calculated by WBM model which shows good agreement with the experimental results and the analytical results of other researchers. Natural frequencies of cylindrical shells with other boundary conditions have also been calculated and the results are compared with the finite element method which also shows good agreement. Effects of the nonuniform rings spacing and nonuniform eccentricity and effects of boundary conditions on the fundamental frequencies and the beam mode frequencies have been studied. Different stiffener distributions are needed to increase the fundamental frequencies and beam mode frequencies for different boundary conditions. WBM model presented in this paper can be recognized as a semianalytical and seminumerical method which is quite useful in analyzing the vibration characteristics of cylindrical shells with nonuniform rings spacing and eccentricity distributions. [DOI: 10.1115/1.4024055]

Keywords: wave based method, cylindrical shell with nonuniform stiffener distribution, free vibration analysis

1 Introduction

Ring stiffened cylindrical shells are widely used in many structure applications such as aeronautic, aerospace, underwater vessel and so on. The free vibration characteristics of cylindrical shells are quite important for use of on-board equipments and so on. Most research focus on cylindrical shells with uniform stiffener distribution because of the convenience of the establishment of mathematical model of the problem, especially convenient for dealing with stiffeners. But in practical engineering applications, stiffeners are sometimes unequally spaced and often with different sizes, such as the existence of intermediate large frame ribs, so a more general model is needed to deal with cylindrical shells with nonuniform stiffener distribution, such as nonuniform eccentricity, unequally spaced and different sizes for ring stiffeners.

Many investigations have been developed to analyze the vibration characteristics of cylindrical shells, e.g., Refs. [1–10]. Energy methods based on the Rayleigh–Ritz procedure and analytical methods are most widely used. Most often cylindrical shells with shear diaphragm-shear diaphragm boundary condition have been investigated because the solution to the governing equations which satisfies boundary conditions can be easily expressed by trigonometric functions. Exponential functions have been chosen for the modal displacements along the axial direction, which are substituted into the equations of motions and then the eight specified boundary conditions are enforced to calculate the natural frequency of cylindrical shells with arbitrary boundary conditions.

In order to effectively enhance the flexural and axial stiffness of cylindrical shells, stiffeners are frequently used. The even spaced rings or stringers are either "smeared out" over the surface of the cylindrical shells or treated as discrete members [11–28]. With rings or stringers "smeared out," the cylindrical shells are treated as orthotropic cylindrical shells [14–18]. The stiffeners must be equally and closely distributed and also with the same depth and width and large errors will be introduced if the stiffeners are large. And also this method is not applicable at mid and high frequencies if the wavelength and the rib spacing are in the same order for neglecting wave transmission and reflection at the discontinuities. Analytical method for the determination of the vibration characteristics of even spaced ring-stiffened shells with shear diaphragm–shear diaphragm (SD-SD) was presented in Refs. [19,20], where rings or stringers are treated as discrete numbers and equations of motions of beams are used to describe the motion of stiffeners. Assuming that the stiffeners uniformly spaced, the displacement at the position of stiffeners are expanded as trigonometric functions which satisfy simply supported boundary conditions to calculate the natural frequencies in Ref. [19]. The method is confined to solve the problem of even spaced ring-stiffened cylindrical shells and simply supported boundary condition. C.H. Hodges et al. [21,22] studied the vibration characteristics of periodic ring-stiffened cylindrical shells with circular T-section ribs according to Bloch's or Floquet's theorem [23]. Recently, Wave propagation method is given in Refs. [24–27] to

[1]Corresponding author.

Contributed by the Design Engineering Division of ASME for publication in the JOURNAL OF VIBRATION AND ACOUSTICS. Manuscript received December 11, 2012; final manuscript received February 25, 2013; published online June 19, 2013. Assoc. Editor: Marco Amabili.

study the vibration characteristics of cylindrical shell, with the effects of ring stiffeners "smeared out" over the surface of the shell in Refs. [25,27]. Beam function with shear diaphragm-shear diaphragm (SD-SD), clamped-clamped (C-C) and clamped-shear diaphragm (C-SD) boundary condition is used to approximate the axial mode function of ring-stiffened cylindrical shell. With the stiffeners treated as discrete elements, Ritz method is applied to analyze the free vibration characteristics of simply supported cylindrical shells with nonuniform rings spacing and eccentricity in Ref. [28] and some conclusions have been made.

A wave based method (WBM) was first proposed in Ref. [29] for prediction of the steady-state dynamics analysis of coupled vibro-acoustic systems which enables accurate predictions in the midfrequency range. Wave based method can be understood as a semianalytical and seminumerical method which is computationally less demanding than corresponding element based models. In contrast with the finite element method (FEM), in which the dynamic field variables within each element are expanded in terms of local, nonexact shape functions, usually polynomial approximation, the dynamic field variables in WBM are expressed as wave function expansions. Modeling of the vibro-acoustic coupling between the pressure field in an acoustic cavity with arbitrary shape and the out-of-plane displacement of a flat plate with arbitrary shape was discussed in Ref. [30] and the unbounded domain was discussed in Ref. [31]. The application of the wave based method for the particular case where stress singularities appear in one or more corners of a polygonal plate domain is discussed in Ref. [32].

In this paper, WBM method is extended to analyze free vibration characteristics of cylindrical shells with nonuniform rings spacing and eccentricity distributions for arbitrary boundary conditions. The cylindrical shell is divided into several substructures the motions of which are described by the equations of Donnell–Mushtari theory and the stiffeners are treated as separate substructures the motions of which are described by the equations of annular circular plates. The displacements within each substructure of cylindrical shells are expanded as a set of wave functions obtained in Ref. [19], and those within the stiffener substructure are expanded as a set of wave functions in Ref. [33]. Then boundary conditions and continuity conditions between substructures are used to form the final matrix to calculate the natural frequencies. Compared with traditional wave propagation method in analyzing free vibration characteristics of ring stiffened cylindrical shells, WBM method has a great advantage in dealing with stiffener of arbitrary sizes and arbitrary distributions for arbitrary boundary conditions. Compared with finite element method possessing a significantly greater generality, a better convergence can be obtained by WBM method and also the size of the final matrix formed to calculate the natural frequencies is much smaller than that formed by finite element method. As a semianalytical and seminumerical method, the shape function chosen in WBM method is more convenient to explain the mechanism of wave propagation including vibration transmission and reflection. The first part of this paper reviews the work already done about free vibration of cylindrical shells. WBM model of cylindrical shells with nonuniform rings spacing and eccentricity distribution is described in the second part. Numerical results are discussed in the third part and some conclusions are made in the fourth part.

2 Basic Concept of Wave Based Model

Wave based method (WBM) is developed for steady-state dynamic analysis of cylindrical shells with nonuniform rings spacing and stiffener distribution. In contrast with the finite element method (FEM), in which the dynamic field variables within each element are expanded in terms of local, nonexact shape functions, usually polynomial approximation, the dynamic field variables within each substructure in WBM model are expressed as wave function expansions, which exactly satisfy the governing dynamic equations of the substructure, and then boundary conditions and continuity conditions are utilized to form the final matrix to calculate the natural frequencies. After that, wave function contribution factors used for postprocessing can be determined.

Similar to the finite element method, several steps are needed to construct a WBM model as follows:

(1) Divide the whole model into different substructures. Different governing equations are used for different types of structure, such as beam, plate and shell. Also different physical properties and the positions of the discontinuities where coupling effects occur need to be considered.
(2) Select suitable wave functions for each substructure. The dynamic field variables, such as the displacement, the velocity and so on, can be expanded by the wave functions which can exactly satisfy the governing equations of the substructures.
(3) Form the final matrix to be solved according to boundary conditions and continuity conditions. Eight specified boundary conditions and eight continuity conditions between different substructures, including forces and displacements, are used to form the final matrix.
(4) Solve the final matrix to get the natural frequencies and the wave function contribution factors. The size of the matrix depends on the total number of substructures and the number of wave function contribution factors in each substructure. Compared with traditional element based model, more unknowns exist in the shape functions but the number of substructures is far more less than the number of elements so the final size of matrix formed is much smaller than FEM.
(5) Postprocessing. The dynamic field variables can be obtained with the wave function contribution factors, such as the displacement, stress, strain and so on.

2.1 Substructure Division of Ring-Stiffened Cylindrical Shells. Cylindrical shells and annular circular plates are main types of structures composing the ring-stiffened cylindrical shells and the stiffeners appear as a discontinuity dividing the cylindrical shell into different substructures. As a ring-stiffened cylindrical shell shown in Fig. 1, the total number of stiffeners is N, and the cylindrical shell is divided into $(N+1)$ bays. The cylindrical shell and the stiffeners are made of the same material, so the total number of substructures is $(2N+1)$ with N substructures describing the motions of stiffeners and $(N+1)$ substructures describing the motions of cylindrical shells. Compared with element based method, this method of substructure division has much less elements.

According to Donnell–Mushtari theory, the following equations describe the motion of thin cylindrical shells [1,2]:

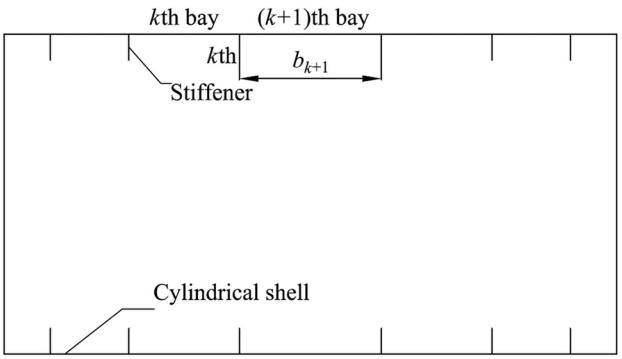

Fig. 1 Ring stiffened cylindrical shells

$$\left.\begin{aligned} L_{11}u + L_{12}v + L_{13}w = 0 \\ L_{21}u + L_{22}v + L_{23}w = 0 \\ L_{31}u + L_{32}v + L_{33}w = 0 \end{aligned}\right\} \tag{1}$$

Differential operators $L_{ij}(i,j=1,2,3)$ are given in Appendix A. u, v, w are the axial, circumferential and outward normal displacements.

The stiffeners are treated as discrete members the motions of which are described by the equations of motions of annular circular plates. Internal stiffening type is considered here which can be applied to external stiffening type easily. The vibrations of annular circular plates with inner radius a_1 and outer radius a (also the radius of the cylindrical shell) with bending and in-plane motions are described in Eq. (2). The axial displacement w_p, radial displacement u_p and circumferential displacement v_p of the plate in polar coordinates are shown in Fig. 2. $\theta_p = \partial w_p/\partial r$ is the twist angle.

$$\left\{\begin{aligned} &\frac{\partial}{\partial r}\left(\frac{\partial u_p}{\partial r}+\frac{u_p}{r}+\frac{1}{r}\frac{\partial v_p}{\partial \theta}\right)-\frac{1-\nu_p}{2r}\frac{\partial}{\partial \theta}\left(\frac{\partial v_p}{\partial r}+\frac{v_p}{r}-\frac{1}{r}\frac{\partial u_p}{\partial \theta}\right)=\frac{\rho_p\left(1-\nu_p^2\right)}{E_p}\frac{\partial^2 u_p}{\partial t^2} \\ &\frac{1}{r}\frac{\partial}{\partial \theta}\left(\frac{\partial u_p}{\partial r}+\frac{u_p}{r}+\frac{1}{r}\frac{\partial v_p}{\partial \theta}\right)+\frac{1-\nu_p}{2}\frac{\partial}{\partial r}\left(\frac{\partial v_p}{\partial r}+\frac{v_p}{r}-\frac{1}{r}\frac{\partial u_p}{\partial \theta}\right)=\frac{\rho_p\left(1-\nu_p^2\right)}{E_p}\frac{\partial^2 v_p}{\partial t^2} \\ &\nabla^4 w_p-\frac{\rho_p\omega^2 h_p}{D_p}w_p=0 \end{aligned}\right. \tag{2}$$

h_p is the plate thickness. E_p, r_p and ν_p are respectively the Young's modulus, density and Poisson's ratio of the annular circular plate. r is the radial coordinate. ω is the angular frequency. $D_p = E_p h_p^3/12(1-\nu_p^2)$ is the flexural rigidity.

2.2 Selection of Wave Functions. For a modal vibration, the axial, circumferential and outward normal displacements of the cylindrical shells and the annular circular plates are usually expressed as a solution expansion

$$\left.\begin{aligned} w &= \sum_{i=1}^{n_s} A_i \Psi_{wi}(x,\phi)\sin(n\phi)e^{-j\omega t} \\ v &= \sum_{i=1}^{n_s} B_i \Psi_{vi}(x,\phi)\cos(n\phi)e^{-j\omega t} \\ u &= \sum_{i=1}^{n_s} C_i \Psi_{ui}(x,\phi)\sin(n\phi)e^{-j\omega t} \end{aligned}\right\} \tag{3}$$

$\Psi_{wi}(x,\phi), \Psi_{vi}(x,\phi), \Psi_{ui}(x,\phi)$ are the structure wave functions which satisfy Eqs. (1) and (2) for a specified circumferential wave number n, A_i, B_i, C_i are the wave contribution factors. n_s is the number of wave functions designating the wave propagation in the axial direction for the cylindrical shell and the radial direction for the annular circular plate.

To insure the WBM model to converge towards the exact solution, the selection of suitable wave function is quite important.

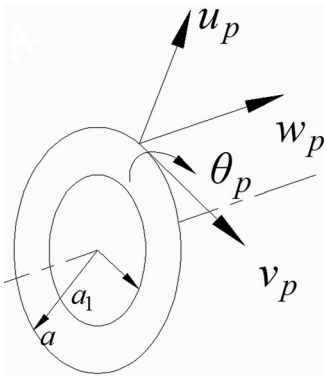

Fig. 2 Displacement of annular circular plate

According to analysis in Ref. [19], a set of wave functions describing the free vibration of cylindrical shell is selected as follows:

$$\begin{aligned} &\Psi_{w1}=\Psi_{v1}=\Psi_{u1}=e^{\lambda_1 x},\quad \Psi_{w2}=\Psi_{v2}=\Psi_{u2}=e^{-\lambda_1 x} \\ &\Psi_{w3}=\Psi_{v3}=\Psi_{u3}=\cos\lambda_2 x,\quad \Psi_{w4}=\Psi_{v4}=\Psi_{u4}=\sin\lambda_2 x \\ &\Psi_{w5}=\Psi_{v5}=\Psi_{u5}e^{\lambda_3 x}\cos\lambda_4 x,\quad \Psi_{w6}=\Psi_{v6}=\Psi_{u6}=e^{\lambda_3 x}\sin\lambda_4 x \\ &\Psi_{w7}=\Psi_{v7}=\Psi_{u7}=e^{-\lambda_3 x}\cos\lambda_4 x,\quad \Psi_{w8}=\Psi_{v8}=\Psi_{u8}=e^{-\lambda_3 x}\sin\lambda_4 x \end{aligned} \tag{4}$$

The wave contribution factors are as follows:

$$\begin{aligned} &B_1=\xi_1 A_1,\quad B_2=\xi_1 A_2,\quad B_3=\xi_2 A_3,\quad B_4=\xi_2 A_4 \\ &B_5=\xi_3 A_5+\xi_4 A_6,\quad B_6=-\xi_4 A_5+\xi_3 A_6 \\ &B_7=\xi_3 A_7-\xi_4 A_8,\quad B_8=\xi_4 A_7+\xi_3 A_8 \end{aligned} \tag{5}$$

$$\begin{aligned} &C_1=\eta_1 A_1,\quad C_2=-\eta_1 A_2,\quad C_3=-\eta_2 A_3,\quad C_4=\eta_2 A_4 \\ &C_5=\eta_3 A_5+\eta_4 A_6,\quad C_6=-\eta_4 A_5+\eta_3 A_6 \\ &C_7=-\eta_3 A_7+\eta_4 A_8,\quad C_8=-\eta_4 A_7-\eta_3 A_8 \end{aligned} \tag{6}$$

In Eqs. (4)–(6), $\lambda_1, \pm i\lambda_1, \pm(\lambda_3 \pm i\lambda_4)$ are character roots to be determined which are given in Appendix B. $\xi_1 \sim \xi_4$ and $\eta_1 \sim \eta_4$ are constant coefficients related to character roots which are also given in Appendix B.

According to Ref. [33], a set of wave functions describing the free vibration of annular circular plate are selected as follows:

$$\begin{aligned} &\psi_{wp1}=J_n(k_{pB}r),\quad \psi_{wp2}=Y_n(k_{pB}r), \\ &\psi_{wp3}=I_n(k_{pB}r),\quad \psi_{wp4}=K_n(k_{pB}r) \\ &\psi_{vp1}=nJ_n(k_{pL}r)/r,\quad \psi_{vp2}=\mathrm{d}J_n(k_{pT}r)/\mathrm{d}r, \\ &\psi_{vp3}=nY_n(k_{pL}r)/r,\quad \psi_{vp4}=\mathrm{d}Y_n(k_{pT}r)/\mathrm{d}r \\ &\psi_{up1}=\mathrm{d}J_n(k_{pL}r)/\mathrm{d}r,\quad \psi_{up2}=nJ_n(k_{pT}r)/r, \\ &\psi_{up3}=\mathrm{d}Y_n(k_{pL}r)/\mathrm{d}r,\quad \psi_{up4}=nY_n(k_{pT}r)/r \end{aligned} \tag{7}$$

The wave contribution factors are as follows:

$$\begin{aligned} &A_1=B_1=B_{1n},\quad A_2=B_2=B_{2n},\quad A_3=B_3=B_{3n},\quad A_4=B_4=B_{4n} \\ &C_1=A_{1n},\quad C_2=A_{2n},\quad C_3=A_{3n},\quad C_4=A_{4n} \end{aligned} \tag{8}$$

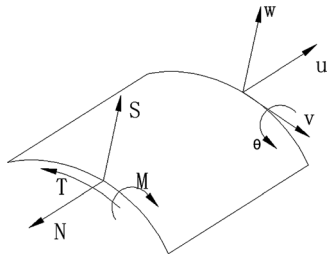

Fig. 3 Displacement constraints and force constraints

$n_s = 8$ is the number of wave functions. J_n, Y_n are, respectively, Bessel functions of the first and the second kind. I_n, K_n are, respectively, modified Bessel functions of the first and second kind. $k_{pB} = (\rho_p \omega^2 h_p / D_p)^{1/4}$ is the plate bending wave number, $k_{pL} = \omega[\rho_p(1-\upsilon_p^2)/E_p]^{1/2}, k_{pT} = \omega[2\rho_p(1+\upsilon_p)/E_p]^{1/2}$ are the wave numbers for in-plane waves in the circular plate. The coefficients $A_{i,n}, B_{i,n} (i = 1,2,3,4)$ are determined from the boundary conditions of the annular circular plates.

2.3 Matrix Formed for Calculating Natural Frequencies. As shown in Fig. 3, the cylindrical shells with arbitrary boundary conditions have four displacement constraints (u, v, w, θ) and four force or moment constraints (M, S, T, N), i.e.,

$$\left.\begin{array}{lll} u = 0 & \text{or} & M = 0 \\ v = 0 & \text{or} & S = 0 \\ w = 0 & \text{or} & T = 0 \\ \theta = 0 & \text{or} & N = 0 \end{array}\right\} \tag{9}$$

where θ designate the twisting angle and M, S, T, N designate bending moment, transverse shear, tangential shear and axial force per unit length of the cylindrical shell and the expressions for M, S, T, N are expressed by Eq. (C6) in Appendix C. Combination of these eight boundary conditions can present arbitrary boundary conditions.

The cylindrical shell with inside stiffeners is divided into two bays by the stiffeners as shown in Fig. 4 where continuity equations must be satisfied.

The displacements of the connection of the adjacent cylindrical shells must be equal, which can lead to the following relationship:

$$u_k^L = u_k^R, \quad v_k^L = v_k^R, \quad w_k^L = w_k^R, \quad \theta_k^L = \theta_k^R \tag{10}$$

At the outer radius of the annular circular plate which is shown in Fig. 4, the continuity conditions of displacements and forces can be expressed as follows:

$$u_{p,k}\big|_{r=a} = w_k^R, \quad v_{p,k}\big|_{r=a} = v_k^R, \quad w_{p,k}\big|_{r=a} = u_k^R, \quad \theta_{p,k}\big|_{r=a} = -\theta_k^R \tag{11}$$

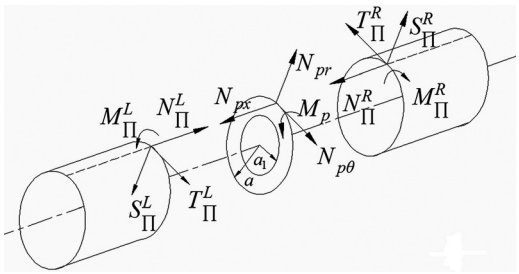

Fig. 4 Interaction forces between stiffener and adjacent bays of cylindrical shells

$$\left.\begin{array}{l} N_k^L = N_{px,k} + N_k^R \\ S_k^L = N_{pr,k} + S_k^R \\ T_k^L = T_k^R - N_{p\theta,k} \\ M_k^L = M_k^R - M_{p,k} \end{array}\right\} \tag{12}$$

The annular circular plates have one free edge at the inner radius (outer radius for the external stiffening type) where boundary conditions are applied as follows:

$$N_{px}\big|_{r=a_1} = 0, \quad N_{pr}\big|_{r=a_1} = 0, \quad N_{p\theta}\big|_{r=a_1} = 0, \quad M_p\big|_{r=a_1} = 0 \tag{13}$$

u_k^L, v_k^L, w_k^L, θ_k^L and u_k^R, v_k^R, w_k^R, θ_k^R denote the axial, circumferential, radial displacement and the twist angle of the left bay and the right bay of the cylindrical shell of the kth stiffener respectively. $u_{p,k}\big|_{r=a}$, $v_{p,k}\big|_{r=a}$, $w_{p,k}\big|_{r=a}$, $\theta_{p,k}\big|_{r=a}$ denote the radial, circumferential, axial displacement and the twist angle of the kth stiffener at the outer radius of the circular plate. M_k^L, S_k^L, T_k^L, N_k^L and M_k^R, S_k^R, T_k^R, N_k^R designate the bending moment, transverse shear, tangential shear and axial force per unit length of the right and the left bay of the cylindrical shell, respectively. M_k^L, $N_{pr,k}$, T_k^L, $N_{px,k}$ and $M_p\big|_{r=a_1}$, $N_{pr}\big|_{r=a_1}$, $N_{p\theta}\big|_{r=a_1}$, $N_{px}\big|_{r=a_1}$ designate the bending moment, transverse shear, tangential shear and axial force per unit length of the kth annular circular plate at the outer and inner radius of the cylindrical shell, respectively.

Combing Eqs. (11) and (13), the eight wave function contributors of the annular circular plate can be expressed by the eight wave function contributors of the adjacent cylindrical shells. The cylindrical shell is divided into $(N+1)$ subsystems which means that there are totally $8(N+1)$ wave contribution factors to be solved. The boundary conditions at both ends of the cylindrical shell and the continuity conditions between the stiffeners and adjacent bays of cylindrical shells can be written and assembled in matrix form for each circumferential mode number n. Omitting the subindex n, the assembled matrix is

$$[\mathrm{K}]\{\mathrm{A}\} = 0 \tag{14}$$

where $\{\mathrm{A}\}$ is the $8(N+1)$ unknown coefficient vectors and

$$[\mathrm{K}] = \begin{bmatrix} [\mathrm{B}_1(0)] & & & & & \\ [\mathrm{D}_1(b_1)] & -[\mathrm{D}_2(0)] & & & & \\ [\mathrm{F}_1(b_1)] & -[\mathrm{F}_2(0)] & & & & \\ & [\mathrm{D}_2(b_2)] & -[\mathrm{D}_3(0)] & & & \\ & [\mathrm{F}_2(b_2)] & -[\mathrm{F}_3(0)] & & & \\ & & \cdots & \cdots & & \\ & & \cdots & \cdots & & \\ & & & [\mathrm{D}_N(b_N)] & -[\mathrm{D}_{N+1}(0)] & \\ & & & [\mathrm{F}_N(b_N)] & -[\mathrm{F}_{N+1}(0)] & \\ & & & & [\mathrm{B}_{N+1}(b_{N+1})] \end{bmatrix} \tag{15}$$

For the kth substructure of the cylindrical shell, the 4×8 matrix blocks $[\mathrm{D}_k]$ and $[\mathrm{F}_k]$ designating displacement and force continuity conditions used in Eq. (15) are as follows. For the continuity equations between stiffeners and adjacent bays of cylindrical shells, blocks $[\mathrm{D}_k]$ and blocks $[\mathrm{F}_k]$ are given by

$$[\mathrm{D}_k(x)]_{4\times 8} = \begin{bmatrix} w_{k,1}(x) \cdots w_{k,8}(x) \\ v_{k,1}(x) \cdots v_{k,8}(x) \\ u_{k,1}(x) \cdots u_{k,8}(x) \\ \theta_{k,1}(x) \cdots \theta_{k,8}(x) \end{bmatrix}, \quad k = 1,2,\ldots,N+1 \tag{16}$$

$$[\mathrm{F}_k(x)]_{4\times 8} = \begin{bmatrix} S_{k,1}(x)\cdots S_{k,8}(x) \\ T_{k,1}(x)\cdots T_{k,8}(x) \\ N_{k,1}(x)\cdots N_{k,8}(x) \\ M_{k,1}(x)\cdots M_{k,8}(x) \end{bmatrix}, \quad k = 1,2,\ldots,N+1 \quad (17)$$

The initial and final blocks $[\mathrm{B}_1]$ and $[\mathrm{B}_{N+1}]$ are expressed in terms of displacement and/or forces, depending on the boundary conditions at each end of the cylindrical shell. Combination of eight boundary conditions in Eq. (9) can present arbitrary boundary conditions. Free, clamped and shear-diaphragm boundary conditions are considered here and are given by

Free end (F)

$$[\mathrm{B}_k(x)]_{4\times 8} = \begin{bmatrix} S_{k,1}(x)\cdots S_{k,8}(x) \\ T_{k,1}(x)\cdots T_{k,8}(x) \\ N_{k,1}(x)\cdots N_{k,8}(x) \\ M_{k,1}(x)\cdots M_{k,8}(x) \end{bmatrix}, \quad k = 1, N+1 \quad (18)$$

Clamped end (C)

$$[\mathrm{B}_k(x)]_{4\times 8} = \begin{bmatrix} w_{k,1}(x)\cdots w_{k,8}(x) \\ v_{k,1}(x)\cdots v_{k,8}(x) \\ u_{k,1}(x)\cdots u_{k,8}(x) \\ \theta_{k,1}(x)\cdots \theta_{k,8}(x) \end{bmatrix}, \quad k = 1, N+1 \quad (19)$$

Shear-diaphragm (SD)

$$[\mathrm{B}_k(x)]_{4\times 8} = \begin{bmatrix} w_{k,1}(x)\cdots w_{k,8}(x) \\ v_{k,1}(x)\cdots v_{k,8}(x) \\ N_{k,1}(x)\cdots N_{k,8}(x) \\ M_{k,1}(x)\cdots M_{k,8}(x) \end{bmatrix}, \quad k = 1, N+1 \quad (20)$$

$[\mathrm{B}_1], [\mathrm{B}_N{+}1], [\mathrm{D}_k], [\mathrm{F}_k](k = 1 \sim N+1)$ are given in Appendix C. $\Phi_k, 1(\Phi = w, v, u, \theta, S, T, N, M)$ designate the values of field variables at the position x of the kth bay of cylindrical shell. b_k designates the length of the kth bay.

2.4 Solution of the Matrix and Postprocessing. When analyzing the free vibration characteristic of ring-stiffened cylindrical shell, the value of the determinant of [K] is calculated for a sequence of trial values of frequency until a sign change is met, then the zero of the determinant is located by iterative interpolation. After a natural frequency has been accurately calculated, the solution to the homogeneous equations (Eq. (14)), normalized by taking $A_N{+}1, 8 = 1$, can be calculated and the mode shape can be obtained.

3 Numerical Results and Discussion

3.1 Cylindrical Shells With Uniform Ring Spacing and Eccentricity. The WBM model is first utilized to calculate the natural frequencies of two ring-stiffened cylindrical shells with C-C, C-SD, SD-SD, C-F, SD-F, F-F boundary conditions. The geometry and material properties of the two shells denoted as model M1 and model M2 which are given in Table 1. Both of the two shells are with external stiffeners of rectangular cross section. Three kinds of shells with stiffeners of different depths are calculated in model M1. The cylindrical shells and the stiffeners have the same materials in both model M1 and model M2. The WBM results are compared with the analytical results already done in relevant references and also FEM results.

The finite element package ANSYS is used to calculate natural frequencies of model M1 and model M2. Both the cylindrical shells and the stiffeners are modeled with shell63 element. In order to ensure the convergence of results calculated by FEM, M1 model with $d_R = 0.00291$ is modeled with three different meshes as shown in Table 2 and the natural frequencies of vibrations modes $m = 1$, $n = 1{\sim}6$ (m, n denote the axial half wave number and the circumferential wave number respectively) with SD-SD boundary conditions have been calculated with the results shown in Table 3. The two numbers in Table 2 for cylindrical shell

Table 1 Geometry dimensions and material properties of stiffened cylindrical shells

	Geometry and material properties	
Characteristics	M1 Model	M2 Model
Radius, a(m)	0.1037	0.049759
Length, l(m)	0.4709	0.3945
Thickness, h(m)	0.00119	0.001651
Density, ρ(kg/m^3)	7850	2762
Young's modulus, E(Pa)	2.06×10^{11}	6.895×10^{10}
Poission's ratio, ν	0.3	0.3
Ring width, b_R(m)	0.00218	0.003175
Ring depth, d_R(m)	0.00291,0.00582,0.00873	0.005334
Number of rings, N	14	19
Stiffening type	External	External

Table 2 FEM models with different meshes

	Number of elements		
	Mesh 1	Mesh 2	Mesh 3
Cylindrical shell	100×90	160×120	200×150
Stiffeners	$100\times1\times14$	$160\times1\times14$	$200\times1\times14$
Total number	10400	21440	32800

Table 3 Natural frequencies of M1 model calculated by three different meshes

	Natural frequencies (Hz)		
Mode number	Mesh 1	Mesh 2	Mesh 3
$n=1$	1610	1610.3	1610
$n=2$	690.87	690.85	690.84
$n=3$	555.15	555.04	555.04
$n=4$	875.46	874.94	874.91
$n=5$	1372	1371	1370
$n=6$	1971	1967.5	1967

Table 4 Comparison of circular frequencies of M1 model (rad/s). (*a*) Basdekas and Chi [20]; (*b*) Galletly [14]; (*c*) Wah and Hu [19]; (*d*) Bosor (smeared rings) [12] and (*e*) Gan and Li [27].

d_R(m)	n	(*a*)	(*b*)	(*c*)	(*d*)	(*e*)	FEM	WBM
0.00291	2	4550	4470	4314	4420	4409	4341	4370
	3	3870	3655	3173	3680	3674	3487	3560
	4	6550	5950	4565	6000	6000	5497	5590
	5	10000	9510	7058	9620	9604	8614	8715
0.00582	2	4580	4450	4235		4481	4357	4386
	3	6710	6235	4615		6492	5717	5782
	4	12830	11790	7982		12149	10154	10248
	5	20120	19020	12660		19694	15639	15767
0.00871	2	5040	4885	4378		4954	4659	4689
	3	10330	9500	6651		9873	8193	8269.8
	4	20200	18010	12154		18884	14608	14735
	5	31800	25570	19221		30606	21803	21992

Table 5 Comparison of natural frequencies of M2 model (Hz). (*e*) Gan and Li [27]; (*f*) Jafari and Bagheri [28]; (*g*) Mustafa and Ali [13]; (*h*) Hoppmann [11]; and (*i*) Hoppmann [11].

n	*m*	(*e*)	(*f*)	(*g*)	(*h*)	Experiment (*i*)	WBM
1	1	1216	1199.58	1204			1154.67
	2	3536	3493.59	3498			3325.82
	3	5907	5839.89	5844			5533.53
	4						7538.00
	5						9249.70
2	1	1635	1564.47	1587	1530	1530	1585.07
	2	2176	2113.84	2129	2100	2040	2112.62
	3	3430	3378.17	3386	3330	3200	3298.39
	4				4860	4440	4712.78
	5				6480	6200	6121.56
3	1	4578	4387.59	4462	4230	4080	4156.73
	2	4573	4400.58	4437	4320	4090	4174.51
	3	4788	4595.79	4627	4500	4520	4407.83
	4				5040	5000	4937.64
	5				5760	5700	5707.83
4	1	8781	8377.75	8559	8100		7424.87
	2	8731	8392.63	8482	8100		7403.14
	3	8728	8449.89	8438	8190	7520	7435.08
	4				8280	7800	7580.76
	5					7920	7873.03
5	1	14172	13490.7	13780	13050		11059.28
	2	14119	13508.9	13695	13100		
	3	14069	13555.4	13595	13140		
	4				13230	11400	11087.96
	5						11207.63

denote the number of elements in the circumferential direction and the axial direction respectively and the three numbers for stiffeners denote the number of elements in the circumferential direction, the radial direction and the number of stiffeners in the axial direction, respectively. 10,500, 21,600 and 33,000 nodes are used in mesh 1, mesh 2 and mesh 3, respectively, with each node having six degrees of freedom UX, UY, UZ, ROTX, ROTY and ROTZ designating three translation degrees and three rotational degrees of freedom. Mesh 2 which can achieve both high computation efficiency and adequate converged results is used in the following analysis.

Table 4 shows the comparison of natural frequencies of model M1 between WBM results and the analytical results of Basdekas and Chi [20], Galletly [14], Wah and Hu [19], Bosor [12] and L. Gan and X. B. Li [27] and also with FEM results. From the table we can see that good agreement can be achieved between different methods for most cases while for other cases large differences have been introduced. The reason why large differences exist is mainly due to some simplifications dealing with the stiffeners in different methods. In method (a), a modified variation method is adopted and the motions of the stiffeners are described by the equations of motions of beams. In method (b), the stiffeners are treated as discrete members but the inter-ring displacement is neglected. In method (c), the stiffeners are also treated as discrete members but the eccentricity of the stiffeners with respect to the shell midsurface is neglected. In method (d), the stiffeners are treated by "smeared method" which can only present an accurate solution when the wavelength is small and the stiffeners are with small sizes. In method (e), the stiffeners are also treated by "smeared method" while beam function is used to approximate the axial mode function of ring stiffened cylindrical shells.

Table 5 shows the comparison of natural frequencies of model M2 between WBM results and the experimental results and the analytical results of Hoppmann [11], the analytical results of Mustafa and Ali [13] and the analytical results of Jafari and Bagheri [28] for various modes of vibrations with SD-SD boundary conditions. As we can see from the tables, when the wave number is small, quite good agreement can be achieved between WBM methods and other methods. The differences increase with the increment of the wave number, while in all the cases WBM results and the experimental results agree quite well. The reason is that the wave length decreases with the increment of the wavenumber and either the stiffener is treated with "smeared method" or treated as discrete members with the motions of stiffener described by the equations of motions of beams can both introduced errors while WBM model is much more exact in such cases.

Table 6 shows comparison between WBM results of M1 model for $d_R = 0.00291$m with C-C, C-SD, SD-SD, C-F, SD-F, F-F boundary conditions. Good agreements have been achieved which shows that WBM model has adequate accuracy to determine the natural frequencies of ring stiffened cylindrical shells with arbitrary boundary conditions.

3.2 Cylindrical Shells With Nonuniform Ring Spacing and Eccentricity. Numerical calculations have been performed here to study the effects of nonuniform rings spacing and nonuniform stiffeners eccentricity distribution, separately and simultaneously.

Table 6 Comparison of natural frequencies of M1 model

Mode		C-C(Hz)			SD-SD(Hz)			C-SD(Hz)		
		FEM	WBM	Error	FEM	WBM	Error	FEM	WBM	Error
m=1	*n*=1	2005.8	2010.3	0.22%	1610.3	1614.1	0.24%	1786.2	1790.2	0.22%
	n=2	1105.5	1109.8	0.39%	690.9	695.5	0.67%	900.8	905.2	0.49%
	n=3	784.7	793.7	1.15%	555.0	566.5	2.07%	658.9	669.0	1.53%
	n=4	950.6	964.5	1.46%	874.9	889.6	1.68%	904.3	918.7	1.59%
	n=5	1396.0	1412.1	1.15%	1371.0	1387.1	1.17%	1379.7	1396.1	1.19%
	n=6	1977.9	1995.7	0.90%	1967.5	1985.3	0.90%	1971.1	1989.0	0.91%
Mode		F-F(Hz)			SD-F(Hz)			C-F(Hz)		
		FEM	WBM	Error	FEM	WBM	Error	FEM	WBM	Error
m=1	*n*=1	3155.0	3122.2	1.04%	2249.1	2254.2	0.23%	2282.0	2287.4	0.24%
	n=2	1483.0	1488.6	0.38%	1044.0	1048.8	0.46%	1221.8	1226.5	0.38%
	n=3	882.7	892.7	1.13%	682.7	693.5	1.58%	818.7	820.2	0.18%
	n=4	925.5	941.1	1.69%	888.8	903.8	1.69%	935.6	950.3	1.57%
	n=5	1374.0	1390.2	1.18%	1371.8	1388.3	1.20%	1383.0	1400.0	1.23%
	n=6	1968.7	1986.5	0.90%	1968.0	1985.9	0.91%	1972.4	1990.2	0.90%

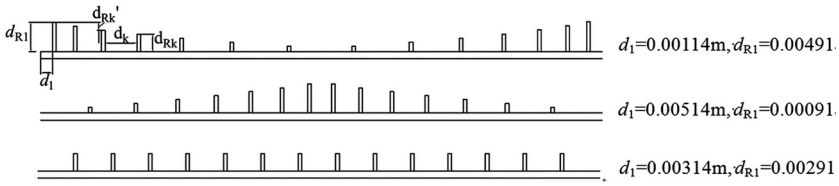

Fig. 5 Uniform and nonuniform rings spacing and eccentricity distribution

M1 model with $d_R = 0.00291$ m with uniform stiffener distribution is considered here, whose properties are shown in Table 1. Some cases of nonuniform rings spacing and nonuniform stiffener distribution are shown in Fig. 5, for which cases the total stiffener mass maintain constant with that of M1 model with evenly rings spacing and equally depth for all stiffeners.

Equating the mass of stiffeners in uniform and nonuniform distributions, a second-order equation corresponding to d_{Rk}' can be obtained as follows [28]:

$$\frac{1}{N}\left(\frac{1}{a+d_{R1}+h/2}\right)^2\sum_{k=1}^{N}d_{Rk}'^2+\frac{2}{N}\left(\frac{1}{a+d_{R1}+h/2}\right)\sum_{k=1}^{N}d_{Rk}' - \frac{2(a+h/2)(d_0-d_{R1})}{(a+d_{R1}+h/2)^2}-\frac{(d_0^2-d_{R1}^2)}{(a+d_{R1}+h/2)^2}=0 \tag{21}$$

Here the difference d_R' between the depths of adjacent stiffeners is considered to maintain constant and the nonuniform eccentricity is symmetrically distributed about the midsection of the shell. Select a value of d_{R1} and a distribution function of d_{Rk}, d_{Rk}' can be determined by solving Eq. (21). The depth of each stiffener can be obtained as follows:

$$d_{Rk}' = \begin{cases} (k-1)d_R' & k \le N/2 \\ (N-k)d_R' & k > N/2 \end{cases} \tag{22}$$

$$d_{Rk} = d_{R1} + d_{Rk}' \tag{23}$$

Similarly, the nonuniform spacing is considered to be symmetrical distributed about the midsection of the shell and the differences between the lengths of adjacent bays of cylindrical shell maintain constant, the nonuniform distribution can be obtained by selecting a value of d_1. The spacing of the kth bay of cylindrical shell can be obtained as follows:

$$d' = \frac{L-(N+1)*d_1}{N^2/4} \tag{24}$$

$$d_k = \begin{cases} d_1+(k-1)d' & k \le N/2 \\ d_1+(N+1-k)d' & k > N/2 \end{cases} \tag{25}$$

In the above equations, d_1 denotes the first ring spacing at the left end and d_{R1} denotes the depth of the first stiffener at the left end. d' denotes the differences between the lengths of adjacent bays of cylindrical shells and d_R' denotes the differences between the depths of adjacent stiffeners. d_{Rk}' denotes the differences between the depths of the kth stiffener and the first stiffener. d_{Rk} and d_k denote the depth of the kth stiffener and the length of kth bay of cylindrical shell, respectively. d_0 denotes the depth of the stiffeners of uniform eccentricity distribution.

For $d_1 < 0.00314$, the rings are closely spaced at the two ends of the cylindrical shell and on the other hand for $d_1 > 0.00314$, the rings are compressed in the midsection of the cylindrical shell. For $d_{R1} > 0.00291$, the eccentricities of the stiffeners at the two ends are larger than those in the midsection and for $d_{R1} < 0.00291$, the eccentricities of the stiffeners at the two ends are smaller than those in the midsection. For $d_1 = 0.00314$ and $d_{R1} = 0.00291$, it denotes uniformly rings spacing and eccentricity distribution. In the following calculation, $d_1 = 0.00114 \sim 0.00514$ and $d_{R1} = 0.00091 \sim 0.00491$.

Figures 6(*a*)–6(*c*) shows the variations of natural frequencies $(m = 1, n = 1 \sim 6)$ of cylindrical shells with respect to the depth (d_{R1}) of the first stiffener with SD-SD, F-F, SD-F boundary conditions. Here the rings spacing is uniform and only the effect of nonuniform eccentricity is considered. It should be noted that decrement of the depth of the first stiffener increase the mass and stiffness in the midsection of the cylindrical shell and decrease them at the two ends.

For the three kinds of boundary conditions, the fundamental frequencies all occur at mode $m = 1$, $n = 3$ except when $d_{R1} = 0.00491$ for SD-F boundary condition for which case the fundament frequency mode changes from $m = 1$, $n = 3$ to $m = 1$, $n = 4$. Increment of the depth of the first stiffener lowers the fundamental frequencies for SD-SD boundary conditions and for other two boundary conditions the fundament frequencies first decrease and then increase with the increment of the depth of the first stiffener and the lowest fundamental frequencies both occur when $d_1 = 0.00314$ and $d_{R1} = 0.00291$, which denotes uniformly rings spacing and eccentricity distribution.

From Fig. 6, we can see that for SD-SD and SD-F boundary conditions, increment of the depth of the first stiffener leads to increment of natural frequencies of the beam mode $(m = 1, n = 1)$ while for F-F boundary conditions it leads to the decrement of natural frequencies of the beam mode. Also the natural frequencies of beam mode with F-F boundary conditions are the highest among the three kinds of boundary conditions and those with SD-SD boundary conditions are the lowest.

Figures 7(*a*)–7(*c*) shows the variations of fundamental frequencies with respect to the depth of the first stiffener for given d_1 with SD-SD, F-F, SD-F boundary conditions. For SD-SD boundary condition, increment of the depth of the first stiffener lower the fundamental frequencies and increment of the first ring spacing increase the fundamental frequencies from which we can make a conclusion that the cylindrical shells get the highest fundamental frequency when $d_{R1} = 0.00091$ and $d_1 = 0.0514$, in another word, more mass concentrated in the midsection of the cylindrical shells, the higher the fundamental frequencies are. For the other two kinds of boundary conditions, the fundamental frequencies first increase and then decrease with respect to the increment of the depth of the first stiffener but the fundamental frequencies not always get the lowest value when rings spacing and eccentricity are uniformly distributed which depends on the value of d_1. Natural frequency curve crossing is observed which shows that the cylindrical shells get the lowest fundamental frequencies when $d_1 = 0.0114$ before the intersection point and get the lowest fundamental frequencies when $d_1 = 0.0514$ after the intersection point.

Figures 8(*a*)–8(*c*) shows the variations of beam mode frequencies with respect to the depth of the first stiffener for given d_1 with SD-SD, F-F, SD-F boundary conditions. We can see from

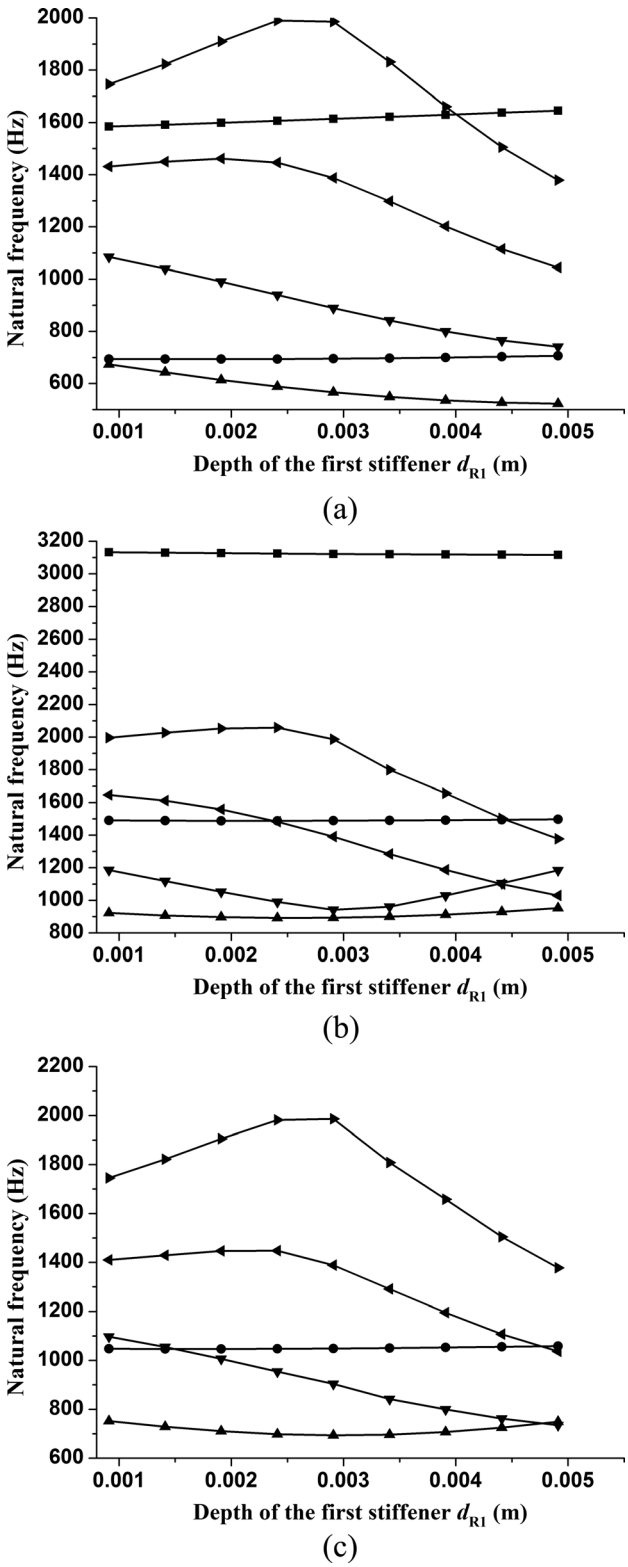

Fig. 6 Natural frequency variations versus the depth of the first stiffener of equally rings spacing ($d_1 = 0.00314$) and nonuniformly eccentricity distribution with SD-SD, SD-F, F-F boundary conditions: (*a*) SD-SD (*b*) F-F (*c*) SD-F —■— n = 1 —•— n = 2 —▲— n = 3 —▼— n = 4 —◀— n = 5 —▶— n = 6

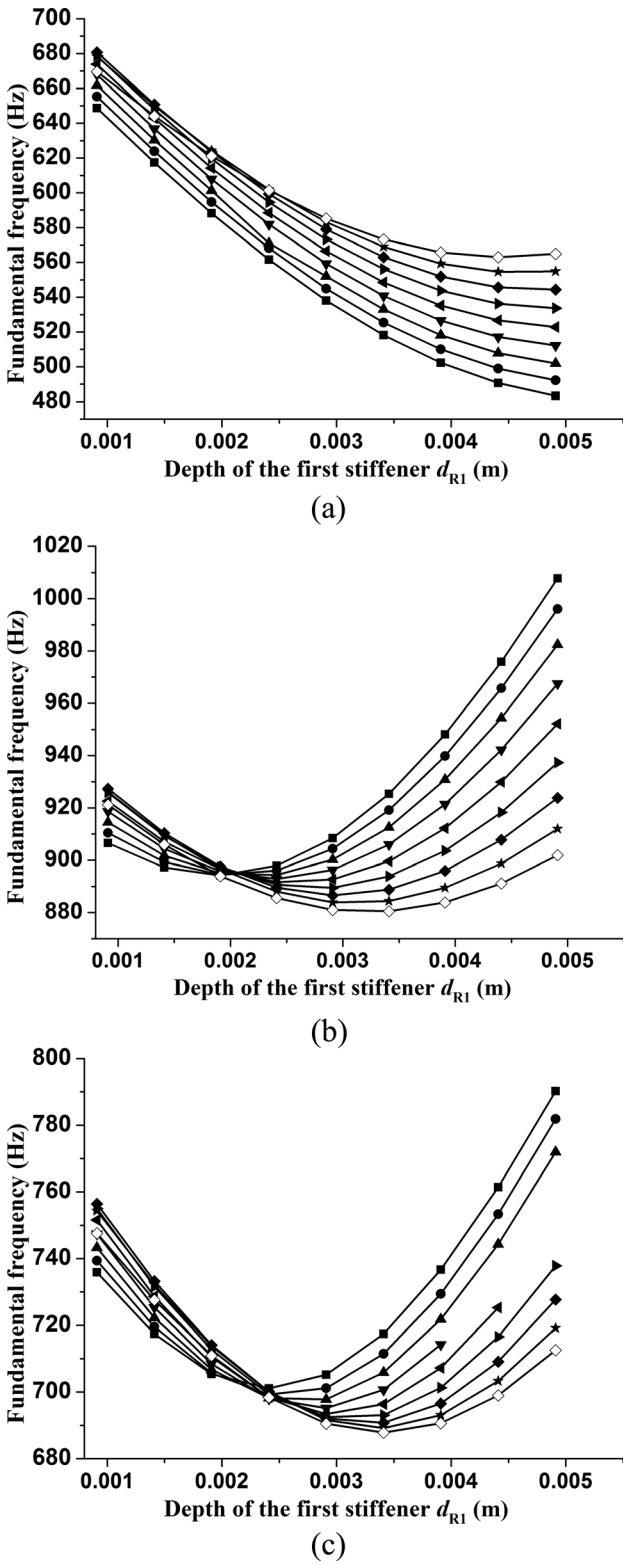

Fig. 7 Fundamental frequency variations versus the depth of the first stiffener for given d_1 with SD-SD, F-F, SD-F boundary conditions: (*a*) SD-SD (*b*) F-F (*c*) SD-F —■— $d_1 = 0.0114$ —•— $d_1 = 0.0164$ —▲— $d_1 = 0.0214$ —▼— $d_1 = 0.0264$ —◀— $d_1 = 0.0314$ —▶— $d_1 = 0.0364$ —◆— $d_1 = 0.0414$ —★— $d_1 = 0.0464$ —◇— $d_1 = 0.0514$

Fig. 7 that for SD-SD boundary conditions the beam mode frequencies increase with the increment of depth of the first stiffener and decrease with the increment of the first ring spacing from which we can make a conclusion that the cylindrical shells get the highest beam mode frequency when $d_{R1} = 0.00491$ and $d_1 = 0.0114$ which means that the less the mass distributed in the

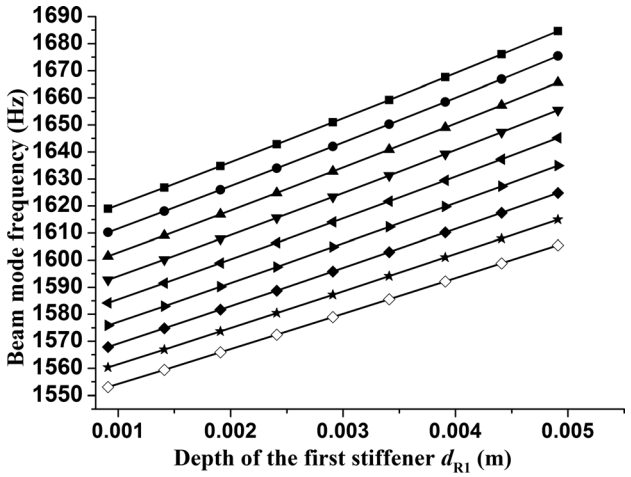

(a)

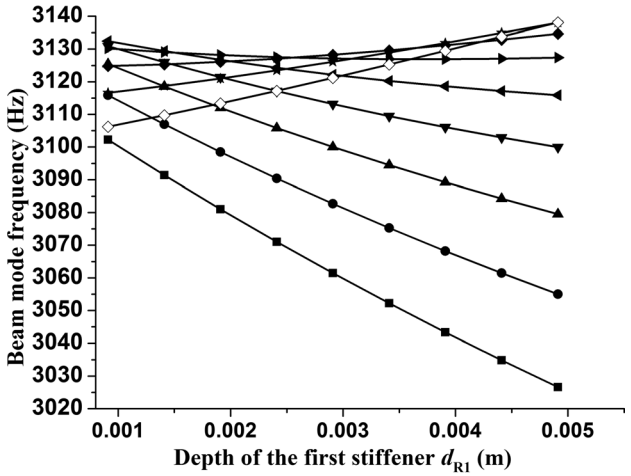

(b)

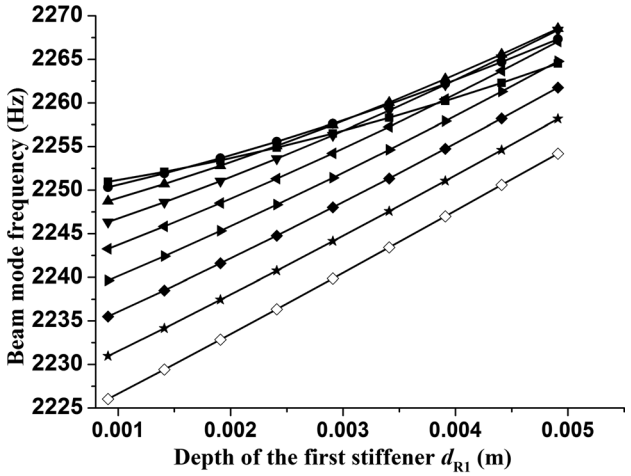

(c)

Fig. 8 Beam mode frequency variations versus the depth of the first stiffener for given d_1 with SD-SD, F-F, SD-F boundary conditions: (*a*) SD-SD (*b*) F-F (*c*) SD-F —■— $d_1 = 0.0114$ —•— $d_1 = 0.0164$ —▲— $d_1 = 0.0214$ —▼— $d_1 = 0.0264$ —◀— $d_1 = 0.0314$ —▶— $d_1 = 0.0364$ —◆— $d_1 = 0.0414$ —★— $d_1 = 0.0464$ —◇— $d_1 = 0.0514$

midsection of the cylindrical shell, the higher the beam mode frequencies are, which is opposite to the variations of the fundamental frequencies with respect to the mass distribution. This conclusion is the same with Jafari and Bagheri [28] where the reason is explained by energy theory. In the beam mode, the shape of stiffeners remain circular and the strain energy of stiffeners does not affect the total energy of the system and only the kinetic energy of stiffeners contributes in the total energy; therefore decrement of mass distribution in the midsection of the shell reduces the kinetic energy and raises the beam mode natural frequency. For F-F boundary condition, the effects of nonuniform ring spacing and eccentricity distribution is rather complicated but a conclusion can be made that the cylindrical shells get the lowest beam mode frequency when $d_{R1} = 0.00491$ and $d_1 = 0.0114$ and get the highest beam mode frequency when $d_{R1} = 0.00491$ and $d_1 = 0.0514$. For SD-F boundary condition, beam mode frequencies increase with the increment of the depth of the first stiffener for given d_1 and before the first intersection point $d_{R1} = 0.00241$ the beam mode frequencies decrease with the increment of the first spacing and after that point the beam mode frequencies first decrease then increase. The cylindrical shells get the highest beam mode frequency when $d_{R1} = 0.00491$ and $d_1 = 0.0214$ and get the lowest beam mode frequency when $d_{R1} = 0.00091$ and $d_1 = 0.0414$.

3.3 Effects of Boundary Conditions on Cylindrical Shells With Nonuniform Rings Spacing and Eccentricity. From the above analysis we can see that boundary conditions have an important effect on the beam mode frequencies and fundamental frequencies of cylindrical shells with nonuniform rings spacing and eccentricity distribution. Here C-C boundary condition is first considered, and then the boundary conditions are released simultaneously at the two ends gradually to consider the effects of boundary conditions on the vibration characteristics of cylindrical shells. The natural frequencies of three models are calculated here which is shown in Fig. 5 and they are denoted as M1 Model 1, M1 Model 2 and M1 Model 3, respectively. The fundamental frequencies are shown in Table 7 and the beam mode frequencies are shown in Table 8. The two numbers in the bracket in Table 7 denote the axial half wave number and the circumferential wave number, respectively.

We can see from Table 7 that M1 Model 2 always gets the highest fundamental frequency and M1 Model 1 always gets the lowest fundamental frequency except when $u = T = S = M = 0$. For M1 Model 2, $m = 1$, $n = 3$ always appears as the fundamental frequency mode except when $N = v = S = M = 0$ and $m = 1$, $n = 4$ appears as the fundamental frequency mode in some cases for M1 Model 1.

The axial displacement constraint has the largest effects on the fundamental frequencies. Release of the axial displacement constraint decreases the fundamental frequencies sharply and does not change the vibration modes most of which still appear as $m = 1$, $n = 3$. Release of other three kinds of boundary conditions decrease the fundamental frequencies much less and lead to the fundamental frequency mode switching from $m = 1$, $n = 3$ to $m = 1$, $n = 2$ or $m = 1$, $n = 4$ for some cases.

From Table 8 we can see that the effects of boundary conditions on beam mode frequencies are rather complicated. Different rings spacing and eccentricity distributions are needed to increase the beam mode frequency for different boundary conditions. M1 Model 1 always gets the highest beam mode frequency when the circumferential displacement constraint is imposed except for C-C boundary condition.

Release of the circumferential displacement constraint can increase the beam mode frequencies rapidly. Release of the other three kinds of displacement constraints will decrease the beam mode and release of the axial displacement constraint lower the beam mode frequency more than the other two. A conclusion can be made that the circumferential displacement constraint has the largest effects on the beam mode frequencies of the cylindrical shells, and the effects of the axial displacement constraint is larger than the other two.

Table 7 Fundamental frequencies with different boundary conditions

Boundary condition		Fundamental frequency (Hz)		
		M1 model 1	M1 model 2	M1 model 3
C-C	$u=v=w=\theta=0$	710.369(1,4)	869.084(1,3)	793.693(1,3)
One boundary condition released	$N=v=w=\theta=0$	489.112(1,3)	674.216(1,3)	571.517(1,3)
	$u=T=w=\theta=0$	710.160(1,4)	842.905(1,3)	770.544(1,3)
	$u=v=S=\theta=0$	709.458(1,4)	865.559(1,3)	789.784(1,3)
	$u=v=w=M=0$	709.833(1,4)	866.113(1,3)	790.518(1,3)
Two boundary conditions released	$N=T=w=\theta=0$	488.939(1,3)	672.183(1,3)	570.852(1,3)
	$N=v=S=\theta=0$	485.590(1,3)	671.791(1,3)	568.789(1,3)
	$N=v=w=M=0$ (SD-SD)	483.323(1,3)	669.668(1,3)	566.477(1,3)
	$u=T=S=\theta=0$	701.333(1,4)	1305.736(1,3)	852.117(1,4)
	$u=T=w=M=0$	690.939(1,3)	798.868(1,3)	730.671(1,3)
	$u=v=S=M=0$	709.452(1,4)	865.205(1,3)	789.447(1,3)
Three boundary conditions released	$N=T=S=\theta=0$	624.969(1,4)	928.643(1,3)	849.354(1,4)
	$N=T=w=M=0$	476.919(1,3)	655.691(1,3)	557.706(1,3)
	$N=v=S=M=0$	483.280(1,3)	570.729(1,2)	566.456(1,3)
	$u=T=S=M=0$	1309.268(1,3)	1305.412(1,3)	1121.270(1,4)
Four boundary conditions released	$N=T=S=M=0$ (F-F)	622.777(1,4)	921.218(1,3)	847.124(1,4)

Table 8 Beam mode frequencies with different boundary conditions

Boundary condition		Beam mode natural frequency (Hz)		
		M1 model 1	M1 model 2	M1 model 3
C-C	$u=v=w=\theta=0$	2109.405	1923.436	2010.241
One boundary condition released	$N=v=w=\theta=0$	1685.649	1553.840	1614.918
	$u=T=w=\theta=0$	4053.764	4114.167	4100.927
	$u=v=S=\theta=0$	2106.321	1920.270	2006.712
	$u=v=w=M=0$	2107.066	1920.901	2007.418
Two boundary conditions released	$N=T=w=\theta=0$	3398.049	3520.205	3497.146
	$N=v=S=\theta=0$	1685.143	1553.434	1614.483
	$N=v=w=M=0$ (SD-SD)	1684.613	1553.038	1614.050
	$u=T=S=\theta=0$	3823.196	3804.443	3879.559
	$u=T=w=M=0$	3925.962	3931.617	3991.735
	$u=v=S=M=0$	2106.192	1920.045	2006.462
Three boundary conditions released	$N=T=S=\theta=0$	3027.103	3106.542	3122.503
	$N=T=w=M=0$	3207.836	3325.436	3320.550
	$N=v=S=M=0$	1684.610	1553.038	1614.050
	$u=T=S=M=0$	3823.178	3804.428	3879.551
Four boundary conditions released	$N=T=S=M=0$ (F-F)	3026.607	3106.211	3122.168

4 Conclusions

Wave based method (WBM) which can be recognized as a semianalytical and seminumerical method presented in this paper is quite useful in analyzing the free vibration characteristics of cylindrical shells with nonuniform rings spacing and stiffener distribution for arbitrary boundary conditions. The ring-stiffened cylindrical shells can be divided into different substructures according to the type of the structure. The motion of each bay of cylindrical shell is described by the equations of Donnell–Mushtari theory and the motions of the stiffeners are described by the equations of motion of annular circular plate. In contrast with the finite element method (FEM), in which the dynamic field variables within each element are expanded in terms of local, non-exact shape functions, usually polynomial approximation, the dynamic field variables within each substructure in WBM are expressed as wave function expansions, which exactly satisfy the governing dynamic equations of the substructure. Numerical results show good agreement with experimental results and analytical results of other researchers for shear diaphragm-shear diaphragm boundary condition and also show good agreement with FEM results for other boundary conditions.

Effects of the nonuniform rings spacing and eccentricity distribution on fundamental frequencies and beam mode frequencies of ring-stiffened cylindrical shells have been studied. For SD-SD boundary conditions, more mass concentrated in the midsection of the cylindrical shells, the higher the fundamental frequencies are while the lower the beam mode frequencies are. For F-F and SD-F boundary conditions, the effects are a little complicated. Numerical results of the effects of boundary conditions show that the axial displacement constraint has the largest effects on fundamental frequencies and the circumferential displacement constraint has the largest effects on beam mode frequencies. Release of the axial displacement constraint decreases the fundamental frequencies sharply and release of the circumferential displacement constraint increases the beam mode frequencies rapidly.

Acknowledgment

All the work in this paper obtains great support from the National Natural Science Foundation of China (51179071) and the Fundamental Research Funds for the Central Universities, HUST: 2012QN056.

Appendix A

The differential operators in Eq. (1) are as follows:

$$L_{11} = \frac{\partial^2}{\partial x^2} + \frac{1-\nu}{2}\frac{\partial^2}{\partial \phi^2} - \frac{\rho(1-\nu^2)a^2}{E}\frac{\partial^2}{\partial t^2}$$

$$L_{22} = \frac{1-\nu}{2}\frac{\partial^2}{\partial x^2} + \frac{\partial^2}{\partial \phi^2} - \frac{\rho(1-\nu^2)a^2}{E}\frac{\partial^2}{\partial t^2}$$

$$L_{33} = 1 + \beta\left(\frac{\partial^4}{\partial x^4} + 2\frac{\partial^4}{\partial x^2 \partial \phi^2} + \frac{\partial^4}{\partial \phi^4}\right) + \frac{\rho(1-\nu^2)a^2}{E}\frac{\partial^2}{\partial t^2}$$

$$L_{12} = L_{21} = \frac{1+\nu}{2}\frac{\partial^2}{\partial x \partial \theta}, \quad L_{13} = L_{31} = \nu\frac{\partial}{\partial x}, \quad L_{23} = L_{32} = \frac{\partial}{\partial \phi}$$

The radius of the cylindrical shell is designated by a, and the thickness by h. $b = h^2/12a^2$, The axial and circumferential coordinates are x, ϕ, $x = \bar{x}/a$. The mass density of the shell's material is designated by ρ, Young's modulus by E and Poission's ratio by ν.

Appendix B

For modal vibration of cylindrical shell with a specified circumferential wave number n, the general solution to Eq. (1) can be written as

$$\left.\begin{aligned} w &= Ae^{\lambda x}\sin n\phi \cos \omega t \\ v &= Be^{\lambda x}\cos n\phi \cos \omega t \\ u &= Ce^{\lambda x}\sin n\phi \cos \omega t \end{aligned}\right\} \tag{B1}$$

where λ is a characteristic root to be determined, ω is circular frequency and ϕ is circumferential coordinate angle.

Substituting Eq. (B1) to Eq. (1) leads to three homogenous equations for the three constants A, B, C. For nontrivial solution, the determinant of their coefficients must vanish, which give the following fourth-degree equation in λ^2.

$$\lambda^8 + g_6\lambda^6 + g_4\lambda^4 + g_2\lambda^2 + g_0 = 0 \tag{B2}$$

where

$$g_6 = \left(\frac{3-\nu}{1-\nu}\right)\Omega^2 - 4n^2$$

$$g_4 = 6n^4 - \frac{3(3-\nu)}{1-\nu}n^2\Omega^2 + \frac{2}{1-\nu}\Omega^4 + \frac{1}{\beta}(1-\nu^2-\Omega^2)$$

$$g_2 = \frac{n^2\Omega^2}{1-\nu}[3(3-\nu)n^2 - 4\Omega^2] - 4n^6 + \frac{\Omega^2}{\beta}\left(3 + 2\nu + 2n^2 - \frac{3-\nu}{1-\nu}\Omega^2\right)$$

$$g_0 = [1/\beta(1-\nu)][(1-\nu)n^2 - 2\Omega^2][\beta n^6 - \Omega^2(1+\beta n^4 + n^2 - \Omega^2)]$$

where Ω is a dimensionless frequency parameter:

$$\Omega^2 = \omega^2 a^2(1-\nu^2)(\rho/E) \tag{B3}$$

For the usual range of parameters and $n \geq 1$, the roots of Eq. (B2) have the form

$$\lambda = \pm\lambda_1, \pm i\lambda_2, \pm(\lambda_3 \pm \lambda_4) \tag{B4}$$

where λ_1, λ_2, λ_3, λ_4 are real quantities. For each root, the ratios C/A, B/A can be determined by Eq. (1), so the general solution of u, v, w can be expressed by eight real constants $A_1 \sim A_8$.

$$\begin{aligned} w = \{&A_1e^{\lambda_1 x} + A_2e^{-\lambda_1 x} + A_3\cos\lambda_2 x + A_4\sin\lambda_2 x \\ &+ A_5e^{\lambda_3 x}\cos\lambda_4 x + A_6e^{\lambda_3 x}\sin\lambda_4 x + A_7e^{-\lambda_3 x}\cos\lambda_4 x \\ &+ A_8e^{-\lambda_3 x}\sin\lambda_4 x\}\sin n\phi\cos\omega t \end{aligned} \tag{B5}$$

$$\begin{aligned} v = \{&A_1\xi_1e^{\lambda_1 x} + A_2\xi_1e^{-\lambda_1 x} + A_3\xi_2\cos\lambda_2 x + A_4\xi_2\sin\lambda_2 x \\ &+ A_5e^{\lambda_3 x}(\xi_3\cos\lambda_4 x - \xi_4\sin\lambda_4 x) + A_6e^{\lambda_3 x}(\xi_4\cos\lambda_4 x \\ &+ \xi_3\sin\lambda_4 x) + A_7e^{-\lambda_3 x}(\xi_3\cos\lambda_4 x + \xi_4\sin\lambda_4 x) \\ &- A_8e^{-\lambda_3 x}(\xi_4\cos\lambda_4 x - \xi_3\sin\lambda_4 x)\}\cos n\phi\cos\omega t \end{aligned} \tag{B6}$$

$$\begin{aligned} u = \{&A_1\eta_1e^{\lambda_1 x} - A_2\eta_1e^{-\lambda_1 x} - A_3\eta_2\sin\lambda_2 x + A_4\eta_2\cos\lambda_2 x \\ &+ A_5e^{\lambda_3 x}(\eta_3\cos\lambda_4 x - \eta_4\sin\lambda_4 x) + A_6e^{\lambda_3 x}(\eta_4\cos\lambda_4 x \\ &+ \eta_3\sin\lambda_4 x) - A_7e^{-\lambda_3 x}(\eta_3\cos\lambda_4 x + \eta_4\sin\lambda_4 x) \\ &+ A_8e^{-\lambda_3 x}(\eta_4\cos\lambda_4 x - \eta_3\sin\lambda_4 x)\}\sin n\phi\cos\omega t \end{aligned} \tag{B7}$$

where

$$\begin{aligned} \xi_1 &= G_1/D_1, \quad \eta_1 = H_1/D_1 \\ \xi_2 &= G_2/D_2, \quad \eta_2 = H_2/D_2 \\ \xi_3 &= \frac{R_1Q_1 + R_2Q_2}{Q_1^2 + Q_2^2}, \quad \eta_3 = \frac{S_1Q_1 + S_2Q_2}{Q_1^2 + Q_2^2} \\ \xi_4 &= \frac{R_2Q_1 - R_1Q_2}{Q_1^2 + Q_2^2}, \quad \eta_4 = \frac{S_2Q_1 - S_1Q_2}{Q_1^2 + Q_2^2} \end{aligned}$$

and

$$\begin{aligned} D_1 &= (1-\nu)\lambda_1^4 + \lambda_1^2[2n^2(\nu-1) + (3-\nu)\Omega^2] + (n^2-\Omega^2)[(1-\nu)n^2 - 2\Omega^2] \\ G_1 &= n[\lambda_1^2(\nu^2+\nu-2) + (1-\nu)n^2 - 2\Omega^2] \\ H_1 &= -\lambda_1[\lambda_1^2\nu(1-\nu) + 2\nu(\Omega^2-n^2) + n^2(1+\nu)] \\ D_2 &= (1-\nu)\lambda_2^4 - \lambda_2^2[2n^2(\nu-1) + (3-\nu)\Omega^2] + (n^2-\Omega^2)[(1-\nu)n^2 - 2\Omega^2] \\ G_2 &= n[-\lambda_2^2(\nu^2+\nu-2) + (1-\nu)n^2 - 2\Omega^2] \\ H_2 &= \lambda_2[\lambda_2^2\nu(1-\nu) - 2\nu(\Omega^2-n^2) - n^2(1+\nu)] \\ Q_1 &= (1-\nu)\{(\lambda_3^2-\lambda_4^2)^2 - 4\lambda_3^2\lambda_4^2\} + (\lambda_3^2-\lambda_4^2)\{2n^2(\nu-1) + (3-\nu)\Omega^2\} + (n^2-\Omega^2)\{(1-\nu)n^2 - 2\Omega^2\} \\ Q_2 &= 4\lambda_3\lambda_4(\lambda_3^2-\lambda_4^2)(1-\nu) + 2\lambda_3\lambda_4\{2n^2(\nu-1) + (3-\nu)\Omega^2\} \\ R_1 &= n\{(\lambda_3^2-\lambda_4^2)(\nu^2+\nu-2) + (1-\nu)n^2 - 2\Omega^2\} \\ R_2 &= 2n\lambda_3\lambda_4(\nu^2+\nu-2) \\ S_1 &= -\lambda_3\{\nu(1-\nu)(\lambda_3^2 - 3\lambda_4^2) + 2\nu(\Omega^2-n^2) + n^2(1+\nu)\} \\ S_2 &= -\lambda_4\{\nu(1-\nu)(3\lambda_3^2 - \lambda_4^2) + 2\nu(\Omega^2-n^2) + n^2(1+\nu)\} \end{aligned}$$

Appendix C

Equations (B5)–(B7) can be written as follows:

$$w(x) = \mathrm{w}(x)\cdot\mathrm{A}, \quad v(x) = \mathrm{v}(x)\cdot\mathrm{A}, \quad u(x) = \mathrm{u}(x)\cdot\mathrm{A} \tag{C1}$$

where

$$\mathrm{w}(x) = [w_1(x) \;\; w_2(x) \;\; \cdots \;\; w_7(x) \;\; w_8(x)] \tag{C2}$$

$$\mathrm{v}(x) = [v_1(x) \;\; v_2(x) \;\; \cdots \;\; v_7(x) \;\; v_8(x)] \tag{C3}$$

$$\mathrm{u}(x) = [u_1(x) \;\; u_2(x) \;\; \cdots \;\; u_7(x) \;\; u_8(x)] \tag{C4}$$

$$\mathrm{A} = [A_1 \;\; A_2 \;\; \cdots \;\; A_7 \;\; A_8] \tag{C5}$$

The twisting angle, forces and moments are given in Ref. [1],

$$\begin{cases} \theta = \dfrac{\partial w}{\partial x} \\ M = \dfrac{D}{a^2}\left(\dfrac{\partial^2 w}{\partial x^2} + \nu\dfrac{\partial^2 w}{\partial \phi^2}\right) \\ S = \dfrac{D}{a^2}\left[\dfrac{\partial^3 w}{\partial x^3} + (2-\nu)\dfrac{\partial^3 w}{\partial x \partial \phi^2}\right] \\ T = \dfrac{Eh}{2a(1+\upsilon)}\left(\dfrac{\partial u}{\partial \phi} + \dfrac{\partial v}{\partial x}\right) \\ N = \dfrac{Eh}{a(1-\upsilon^2)}\left[\dfrac{\partial u}{\partial x} + \nu\left(\dfrac{\partial v}{\partial \phi} + w\right)\right] \end{cases} \tag{C6}$$

Substituting Eqs. (B5)–(B7) to Eq. (C6)

$$w_1 = e^{\lambda_1 x}, \quad w_2 = e^{-\lambda_1 x}, \quad w_3 = \cos\lambda_2 x, \quad w_4 = \sin\lambda_2 x$$
$$w_5 = e^{\lambda_3 x}\cos\lambda_4 x, \quad w_6 = e^{\lambda_3 x}\sin\lambda_4 x, \quad w_7 = e^{-\lambda_3 x}\cos\lambda_4 x, \quad w_8 = e^{-\lambda_3 x}\sin\lambda_4 x$$
$$v_1 = \xi_1 e^{\lambda_1 x}, \quad v_2 = \xi_1 e^{-\lambda_1 x}, \quad v_3 = \xi_2\cos\lambda_2 x, \quad v_4 = \xi_2\sin\lambda_2 x$$
$$v_5 = G_1 e^{\lambda_3 x}, \quad v_6 = G_2 e^{\lambda_3 x}, \quad v_7 = G_3 e^{-\lambda_3 x}, \quad v_8 = G_4 e^{-\lambda_3 x}$$
$$u_1 = \eta_1 e^{\lambda_1 x}, \quad u_2 = -\eta_1 e^{-\lambda_1 x}, \quad u_3 = -\eta_2\sin\lambda_2 x, \quad u_4 = \eta_2\cos\lambda_2 x$$
$$u_5 = F_1 e^{\lambda_3 x}, \quad u_6 = F_2 e^{\lambda_3 x}, \quad u_7 = -F_3 e^{-\lambda_3 x}, \quad u_8 = F_4 e^{-\lambda_3 x}$$
$$\theta_1 = \lambda_1 e^{\lambda_1 x}, \quad \theta_2 = -\lambda_1 e^{-\lambda_1 x}, \quad \theta_3 = -\lambda_2\sin\lambda_2 x, \quad \theta_4 = \lambda_2\cos\lambda_2 x$$
$$\theta_5 = H_1 e^{\lambda_3 x}, \quad \theta_6 = H_2 e^{\lambda_3 x}, \quad \theta_7 = -H_3 e^{-\lambda_3 x}, \quad \theta_8 = H_4 e^{-\lambda_3 x}$$

$$M_1 = \frac{D}{a^2}\delta_1 e^{\lambda_1 x}, \quad M_2 = \frac{D}{a^2}\delta_1 e^{-\lambda_1 x}, \quad M_3 = -\frac{D}{a^2}\delta_2\cos\lambda_2 x, \quad M_4 = -\frac{D}{a^2}\delta_2\sin\lambda_2 x$$
$$M_5 = -\frac{D}{a^2}e^{\lambda_3 x}(\delta_4\sin\lambda_4 x - \delta_3\cos\lambda_4 x), \quad M_6 = \frac{D}{a^2}e^{\lambda_3 x}(\delta_3\sin\lambda_4 x + \delta_4\cos\lambda_4 x)$$
$$M_7 = \frac{D}{a^2}e^{-\lambda_3 x}(\delta_3\cos\lambda_4 x + \delta_4\sin\lambda_4 x), \quad M_8 = -\frac{D}{a^2}e^{-\lambda_3 x}(\delta_4\cos\lambda_4 x - \delta_3\sin\lambda_4 x)$$

$$S_1 = \frac{D}{a^3}\gamma_1 e^{\lambda_1 x}, \quad S_2 = -\frac{D}{a^3}\gamma_1 e^{-\lambda_1 x}, \quad S_3 = \frac{D}{a^3}\gamma_2\sin\lambda_2 x, \quad S_4 = -\frac{D}{a^3}\gamma_2\cos\lambda_2 x$$
$$S_5 = \frac{D}{a^3}e^{\lambda_3 x}(\gamma_3\cos\lambda_4 x - \gamma_4\sin\lambda_4 x), \quad S_6 = \frac{D}{a^3}e^{\lambda_3 x}(\gamma_3\sin\lambda_4 x + \gamma_4\cos\lambda_4 x)$$
$$S_7 = -\frac{D}{a^3}e^{-\lambda_3 x}(\gamma_3\cos\lambda_4 x + \gamma_4\sin\lambda_4 x), \quad S_8 = -\frac{D}{a^3}e^{-\lambda_3 x}(\gamma_3\sin\lambda_4 x - \gamma_4\cos\lambda_4 x)$$

$$T_1 = \frac{D}{a^3}\chi_1 e^{\lambda_1 x}, \quad T_2 = -\frac{D}{a^3}\chi_1 e^{-\lambda_1 x}, \quad T_3 = -\frac{D}{a^3}\chi_2\sin\lambda_2 x, \quad T_4 = \frac{D}{a^3}\chi_2\cos\lambda_2 x$$
$$T_5 = -\frac{D}{a^3}e^{\lambda_3 x}(\chi_4\sin\lambda_4 x - \chi_3\cos\lambda_4 x), \quad T_6 = \frac{D}{a^3}e^{\lambda_3 x}(\chi_4\cos\lambda_4 x + \chi_3\sin\lambda_4 x)$$
$$T_7 = -\frac{D}{a^3}e^{-\lambda_3 x}(\chi_3\cos\lambda_4 x + \chi_4\sin\lambda_4 x), \quad T_8 = -\frac{D}{a^3}e^{-\lambda_3 x}(\chi_3\sin\lambda_4 x - \chi_4\cos\lambda_4 x)$$

$$N_1 = \frac{D}{a^3}\mu_1 e^{\lambda_1 x}, \quad N_2 = \frac{D}{a^3}\mu_1 e^{-\lambda_1 x}, \quad N_3 = \frac{D}{a^3}\mu_2\cos\lambda_2 x, \quad N_4 = \frac{D}{a^3}\mu_2\sin\lambda_2 x$$
$$N_5 = -\frac{D}{a^3}e^{\lambda_3 x}(\mu_4\sin\lambda_4 x - \mu_3\cos\lambda_4 x), \quad N_6 = \frac{D}{a^3}e^{\lambda_3 x}(\mu_4\cos\lambda_4 x + \mu_3\sin\lambda_4 x)$$
$$N_7 = \frac{D}{a^3}e^{-\lambda_3 x}(\mu_3\cos\lambda_4 x + \mu_4\sin\lambda_4 x), \quad N_8 = -\frac{D}{a^3}e^{-\lambda_3 x}(\mu_4\cos\lambda_4 x - \mu_3\sin\lambda_4 x)$$

$$F_1 = \eta_3\cos\lambda_4 x - \eta_4\sin\lambda_4 x, \quad F_2 = \eta_4\cos\lambda_4 x + \eta_3\sin\lambda_4 x$$
$$F_3 = \eta_3\cos\lambda_4 x + \eta_4\sin\lambda_4 x, \quad F_4 = \eta_4\cos\lambda_4 x - \eta_3\sin\lambda_4 x$$

$$G_1 = \xi_3 \cos \lambda_4 x - \xi_4 \sin \lambda_4 x, \quad G_2 = \xi_4 \cos \lambda_4 x + \xi_3 \sin \lambda_4 x$$
$$G_3 = \xi_3 \cos \lambda_4 x + \xi_4 \sin \lambda_4 x, \quad G_4 = -\xi_4 \cos \lambda_4 x + \xi_3 \sin \lambda_4 x$$

$$H_1 = \lambda_3 \cos \lambda_4 x - \lambda_4 \sin \lambda_4 x, \quad H_2 = \lambda_4 \cos \lambda_4 x + \lambda_3 \sin \lambda_4 x$$
$$H_3 = \lambda_3 \cos \lambda_4 x + \lambda_4 \sin \lambda_4 x, \quad H_4 = \lambda_4 \cos \lambda_4 x - \lambda_3 \sin \lambda_4 x$$

$$\delta_1 = \lambda_1^2 - \nu n^2, \quad \delta_2 = \lambda_2^2 + \nu n^2, \quad \delta_3 = \lambda_3^2 - \lambda_4^2 - \nu n^2, \quad \delta_4 = 2\lambda_3\lambda_4$$

$$\gamma_1 = \lambda_1\{\lambda_1^2 - (2-\nu)n^2\}, \quad \gamma_2 = \lambda_2\{\lambda_2^2 + (2-\nu)n^2\}$$
$$\gamma_3 = \lambda_3\{\lambda_3^2 - 3\lambda_4^2 - (2-\nu)n^2\}, \quad \gamma_4 = \lambda_4\{3\lambda_3^2 - \lambda_4^2 - (2-\nu)n^2\}$$

$$\chi_1 = [(1-\nu)/2\beta](n\eta_1 + \xi_1\lambda_1), \quad \chi_2 = [(1-\nu)/2k](n\eta_2 + \xi_2\lambda_2)$$
$$\chi_3 = [(1-\nu)/2\beta](n\eta_3 + \xi_3\lambda_3 - \xi_4\lambda_4), \quad \chi_4 = [(1-\nu)/2k](n\eta_4 + \xi_4\lambda_3 + \xi_3\lambda_4)$$

$$\mu_1 = (1/\beta)\{\eta_1\lambda_1 + \nu(1 - n\xi_1)\}, \quad \mu_2 = (1/\beta)\{-\eta_2\lambda_2 + \nu(1 - n\xi_2)\}$$
$$\mu_3 = (1/\beta)\{\eta_3\lambda_3 - \eta_4\lambda_4 + \nu(1 - n\xi_3)\}, \quad \mu_4 = (1/\beta)(\eta_4\lambda_3 + \eta_3\lambda_4 - \nu n\xi_4)$$

References

[1] Leissa, A. W., 1973, "Vibration of Shell," NASA, Ohio.
[2] Flügge, W., 1973, *Stress in Shells*, Springer, Berlin.
[3] Arnold, R. N., Warburton, G. B., 1949, "Flexural Vibrations of the Walls of Thin Cylindrical Shells Having Freely Supported Ends," Proc. R. Soc. London, Ser. A., **197**(1049), pp. 238–256.
[4] Sharma, C. B., 1974, "Calculation of Natural Frequencies of Fixed-Free Circular Cylindrical Shells," J. Sound Vib., **35**(1), pp. 55–76.
[5] Arnold, R. N., and Warburton, G. B., 1953, "The Flexural Vibrations of Thin Cylinders," Proc. Inst. Mech. Eng., Part A., **167**(1), pp. 62–80.
[6] Forsberg, K., 1963, "Influence of Boundary Conditions on the Modal Characteristics of Thin Cylindrical Shells," J. Acoust. Soc. Am., **35**(11), pp. 1898–1899.
[7] Forsberg, K., 1969, "Axisymmetric and Beam-Type Vibrations of Thin Cylindrical Shells," AIAA J., **7**(2), pp. 221–227.
[8] Warburton, G. B., 1965, "Vibrations of Thin Cylindrical Shells," Proc. Inst. Mech. Eng., Part C: J. Mech. Eng. Sci., **7**(4), pp. 399–407.
[9] Warburton, G. B., and Higgs, J., 1970, "Natural Frequencies of Thin Cantilever Cylindrical Shells," J. Sound Vib., **11**(3), pp. 335–338.
[10] Goldman, R. L., 1974, "Mode Shapes and Frequencies of Clamped-Clamped Cylindrical Shells," AIAA J., **12**(12), pp. 1755–1756.
[11] Hoppmann, W. H., 1958, "Some Characteristics of the Flexural Vibrations of Orthogonally Stiffened Cylindrical Shells," J. Acoust. Soc. Am., **29**(6), pp. 772–772.
[12] Everstine, G. C., 1970, "Ring-Stiffened Cylinder," Proceeding of NSRDC-NASTRAN Colloquium, Washington, DC, January 12–13.
[13] Mustafa, B., and Ali, R., 1989, "An Energy Method for Free Vibration Analysis of Stiffened Circular Cylindrical Shells," Comput. Struct., **32**(2), pp. 335–363.
[14] Galletly, G. D., 1954, "On the In Vacuo Vibrations of Simply Supported Ring-Stiffened Cylindrical Shell," Proceedings of the Second US National Congress of Applied Mechanics, Ann Arbor, MI, June 14–18.
[15] Sewall, J. L., Clary, R. R., and Leadbetter, S. A., 1964, "An Experimental and Analytical Vibration Study of Ring-Stiffened Cylindrical Shell Structure With Various Support Conditions," Report No. NASA TN D-2398.
[16] Sewall, J. L., and Naumann, E. C., 1968, "An Experimental and Analytical Vibration Study of Thin Cylindrical Shells With and Without Longitudinal Stiffeners," Report No. NASA TN D-4705.
[17] Caresta, M., and Kessissoglou, N. J., 2009, "Structural and Acoustic Responses of a Fluid-Loaded Cylindrical Hull With Structural Discontinuities," Appl. Acoust., **70**(7), pp. 954–963.
[18] Caresta, M., and Kessissoglou, N. J., 2011, "Reduction of Hull-Radiated Noise Using Vibroacoustic Optimization of the Propulsion System," J. Ship. Res., **55**(3), pp. 149–162.
[19] Wah, Thein, and Hu, William, C. L., 1968, "Vibration Analysis of Stiffened Cylinders Including Inter-Ring Motion," J. Acoust. Soc. Am., **43**(5), pp. 1005–1016.
[20] Basdekas, N. L., and Chi, M., 1971, "Response of Oddly Stiffened Circular Cylindrical Shell," J. Sound Vib., **17**(2), pp. 187–206.
[21] Hodges, C. H., Power, J., and Woodhouse, J., 1985, "The Low Frequency Vibration of a Ribbed Cylinder, Part 1: Theory," J. Sound Vib., **101**(2), pp. 219–235.
[22] Hodges, C. H., Power, J., and Woodhouse, J., 1985, "The Low Frequency Vibration of a Ribbed Cylinder—Part 2: Observations and Interpretation," J. Sound Vib., **101**(2), pp. 237–256.
[23] Brillouin, L., 1946, *Wave Propagation in Periodic Structures*, McGraw-Hill, New York.
[24] Li, X. B., 2006, "A New Approach for Free Vibration Analysis of Thin Circular Cylindrical Shell," J. Sound Vib., **296**(1–2), pp. 91–98.
[25] Pan, Z., Li, X. B., and Ma, J. J., 2008, "A Study on Free Vibration of a Ring-Stiffened Thin Circular Cylindrical Shell With Arbitrary Boundary Conditions," J. Sound Vib., **314**(1–2), pp. 330–342.
[26] Li, X. B., 2008, "Study on Free Vibration Analysis of Circular Cylindrical Shells Using Wave Propagation," J Sound Vib., **311**(3–5), pp. 667–682.
[27] Gan, L., Li, X. B., and Zhang, Z., 2009, "Free Vibration Analysis of Ring-Stiffened Cylindrical Shells Using Wave Propagation Approach," J. Sound Vib., **326**(3–5), pp. 633–646.
[28] Jafari, A. A., and Bagheri, M., 2006, "Free Vibration of Non-Uniformly Ring Stiffened Cylindrical Shells Using Analytical, Experimental and Numerical Methods," Thin. Walled Struct., **44**(1), pp. 82–90.
[29] Desmet, W., 1998, "A Wave Based Prediction Technique for Coupled Vibro-Acoustic Analysis," Ph.D. thesis, K.U., Leuven, Belgium.
[30] Desmet, W., van Hal, B., Sas, P., and Vandepitte, D., 2002, "A Computationally Efficient Prediction Technique for the Steady-State Dynamic Analysis of Coupled Vibro-Acoustic Systems," Adv. Eng. Software, **33**(7–10), pp. 527–540.
[31] Pluymers, B., Desmet, W., Vandepitte, D., and Sas, P., 2004, "Application of an Efficient Wave-Based Prediction Technique for the Analysis of Vibro-Acoustic Radiation Problems," Comput. Appl. Math., **168**(1–2), pp. 353–364.
[32] Vanmaele, C., Vandepitte, D., and Desmet, W., 2009, "An Efficient Wave Based Prediction Technique for Dynamic Plate Bending Problems With Corner Stress Singularities," Comput. Methods Appl. Mech. Eng., **198**(30–32), pp. 2227–2245.
[33] Tso, Y. K., and Hansen, C. H., 1995, "Wave Propagation Through Cylinder/Plate Junctions," J. Sound Vib., **186**(3), pp. 447–461.